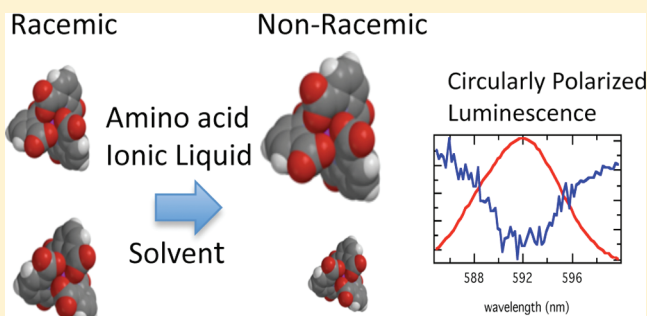


Chiroptical Study of Chiral Discrimination by Amino Acid Based Ionic Liquids

Daniel M. Kroupa, Christopher J. Brown, Laurel M. Heckman, and Todd A. Hopkins*

Department of Chemistry, Butler University, 4600 Sunset Avenue, Indianapolis, Indiana 46208, United States

ABSTRACT: The chiral discrimination ability of amino acid based chiral ionic liquids is studied using chiroptical luminescence techniques. A racemic mixture of dissymmetric europium tris(2,6-pyridinedicarboxylate) complexes are dissolved in five chiral ionic liquids, including L- and D-alanine methyl ester bis(trifluoromethanesulfonimide), L-leucine methyl ester bis(trifluoromethanesulfonimide), L-proline methyl ester bis(trifluoromethanesulfonimide), and tetrabutylammonium L-alanate. Circularly polarized luminescence spectra are measured for the samples over the 283–323 K temperature range. Analysis of the spectroscopic results shows that the amino acid methyl ester chiral ionic liquids show discrimination with a preference (handedness) that corresponds to the stereoisomer (L- vs D-). Most of the chiral ionic liquids show enthalpically dominated discrimination, but L-leucine methyl ester bis(trifluoromethanesulfonimide) shows entropically dominated chiral discrimination.



INTRODUCTION

Affecting and controlling chiral discrimination processes has been a goal of chemists and biochemists for over a century and remains extremely important to a number of industries, including pharmaceutical and agrochemical. Within the past few years, the development of chiral ionic liquids (CILs), low melting point salts with chiral cation and/or anion, has grown considerably over the last 10 years, and this has brought significant interest to their use as chiral solvents in asymmetric processes.^{1–4} One advantage to CILs is that they offer considerable control and flexibility over stereochemical structure and properties simply by the choice of cation–anion pairings.^{5,6} Numerous chiral structural motifs^{1,7–11} have been exploited in the development of CILs, including ionic liquids based upon amino acids.^{12–14} A number of recent studies have demonstrated the use of CILs in chiral discrimination applications such as separations,^{15–18} asymmetric syntheses, and catalysis.^{4,18–22}

The amino acid based CILs are interesting for chiral discrimination applications because they have significant structural diversity based on their different $-R$ groups, do not require asymmetric synthesis, and can be converted to the chiral cation¹² or anion¹³ through relatively simple chemistry. Since the main advantage of using CILs in chiral discrimination applications is the synthetic control one has over their properties, including stereochemistry, a series of amino acid based CILs form an excellent basis for studying the relationship between the chemical and physical properties of CILs and their chiral discrimination ability. The chiral discrimination by amino acid CILs has been demonstrated in previous studies using F-19 NMR and fluorescence spectroscopy,²³ separations,^{18,24} and reactions.^{25,26} However, these studies are limited in the number

of amino acid CILs investigated. This paper presents results of chiral discrimination studies of amino acid based CILs in an attempt to rationalize the relationship between amino acid structure and discrimination.

Table 1 shows structures of the five amino acid CILs that were studied in this paper. Four of the CILs have amino acid methyl ester as the cation with the bis-(trifluoromethanesulfonimide) anion. Therefore, any difference in chiral discrimination between these four can be attributed to the structure of the amino acid, and not chain length of the ester or the anion it is paired with. The amino acid methyl esters include the enantiomeric pair, [L- vs D-AlaC1][Tf₂N], nonpolar (L-LeuC1 and AlaC1), and cyclic (L-ProC1) amino acids. The fifth CIL studied is [TBA][L-Ala], where the amino acid is the anion in the ionic liquid.

One method to measure the chiral discrimination of CILs is through determination of the enantiomeric excess (ee) of a process or reaction (e.g., asymmetric Michael addition²⁷), but purification and separation steps are required to determine the chiral discrimination that occurred. Many studies use F-19 NMR of Mosher's acid²⁸ or fluorescence spectroscopy^{23,29} as a general descriptor of chiral discrimination, but these require the addition of cosolvents. The study in this paper uses a chiroptical spectroscopic technique to determine the chiral discrimination by the CIL solvent. A racemic mixture of luminescent lanthanide complexes, Λ - and Δ -Eu(dpa)₃^{3–} (where dpa = 2,6-pyridinedicarboxylate dianion), is dissolved in the amino acid CIL, and the amount and sense (handedness)

Received: January 11, 2012

Revised: March 9, 2012

Published: March 30, 2012



Table 1. Amino Acid CILs

Cations	Anions
$\left[\begin{array}{c} \text{H}_3\text{C} \\ \\ \text{N}^+\text{H}_3 \\ \\ \text{C} \\ \\ \text{OCH}_3 \end{array} \right]$ <p>L- and D-Alanine methyl ester = AlaC1</p>	$\left[\begin{array}{c} \text{O} \\ \\ \text{F}_3\text{C}-\text{S}-\text{N}^--\text{S}-\text{CF}_3 \\ \\ \text{O} \end{array} \right]$ <p>$[(\text{CF}_3\text{SO}_2)_2\text{N}]^- = \text{Tf}_2\text{N}^-$</p>
$\left[\begin{array}{c} \text{NH}_3^+ \\ \\ \text{CH}_2 \\ \\ \text{CH} \\ \\ \text{OCH}_3 \end{array} \right]$ <p>L-Leucine methyl ester = LeuC1</p>	
$\left[\begin{array}{c} \text{O} \\ \\ \text{C} \\ \\ \text{NH}_2^+ \end{array} \right]$ <p>L-Proline methyl ester = ProC1</p>	
$\left[\begin{array}{c} \text{N}^+ \\ \\ \text{C} \\ \\ \text{C} \\ \\ \text{C} \\ \\ \text{C} \end{array} \right]$ <p>TBA⁺ (tetrabutylammonium ion)</p>	$\left[\begin{array}{c} \text{O} \\ \\ \text{C} \\ \\ \text{NH}_2 \end{array} \right]$ <p>L-Alanate</p>

of chiral discrimination is measured using circularly polarized luminescence (CPL). This allows for the determination of chiral discrimination in one step, without the need for separation or addition of a cosolvent.

The coordination complex, $\text{Eu}(\text{dpa})_3^{3-}$, has trigonal dihedral (D_3) symmetry, and the three bicyclic chelate rings form either a left-handed (Λ) or right-handed (Δ) three-bladed propeller arrangement about the threefold axis. All of the structural chirality in these complexes is derived from the helical distribution of the chelate rings about the lanthanide ion because the individual ligands and their chelate rings have achiral structures. Following standard practice, we label the structural enantiomers of $\text{Eu}(\text{dpa})_3^{3-}$ as Λ or Δ , which refer to the helicity of the chelate rings about the trigonal (C_3) symmetry axis. However, although the Λ enantiomer is defined to have left-handed chirality about its trigonal axis, it has right-handed chirality about each of its three twofold (C_2) symmetry axes. Conversely, the Δ enantiomer is defined to have right-handed chirality about its trigonal axis and left-handed chirality about each of its twofold axes. Therefore, the absolute configuration of an enantiomer is uniquely specified by the label Λ or Δ , but the “handedness” of its structure is dependent upon the choice of reference axis. A space-filling structural representation of the Δ - $\text{Eu}(\text{dpa})_3^{3-}$ enantiomer is shown in Figure 1, with views along the trigonal axis and one of the twofold axes. In solution, the $\text{Eu}(\text{dpa})_3^{3-}$ complexes exist as racemic mixtures of interconverting ($\Lambda \leftrightarrow \Delta$) enantiomers.³⁰ Previous studies have shown that the introduction of a chiral perturbation, such as amino acids, to the $\text{Eu}(\text{dpa})_3^{3-}$ complexes in solution generates a nonracemic (Λ vs Δ) population without changing the coordination environment and fundamental chiroptical properties of the complex.^{31,32}

Circularly polarized luminescence is the emission analogue of circular dichroism (CD), where CPL is the difference in the intensity of left (I_L) and right (I_R) circularly polarized light.

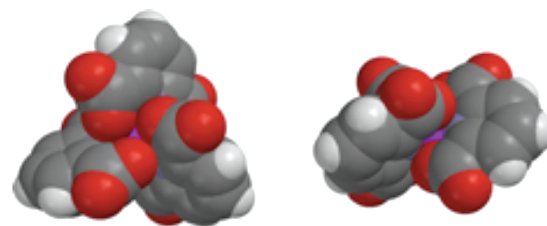


Figure 1. Structural representation of the Δ - $\text{Eu}(\text{dpa})_3^{3-}$ enantiomer. The structure on the left side is viewed along the trigonal symmetry axis, and the structure on the right is viewed along one of the digonal (C_2) symmetry axis.

Since CPL is an emission measurement, it is less likely than CD to suffer from background interference. This is especially important in studies with CILs because even a small intrinsic CD signal from the solvent can overwhelm any CD from probe molecules. In order to compare across samples with different luminescence efficiencies, the most relevant observable in CPL spectra is the emission dissymmetry factor, $g_{\text{em}}(\lambda)$, which is expressed as³³

$$g_{\text{em}}(\lambda) = \frac{2[I_L(\lambda) - I_R(\lambda)]}{I_L(\lambda) + I_R(\lambda)} = \frac{2\Delta I(\lambda)}{I(\lambda)} \quad (1)$$

where $\Delta I(\lambda)$ is the CPL at wavelength λ and $I(\lambda)$ is the total luminescence at wavelength λ . The emission dissymmetry factor can have values that range from +2 to −2.

The $\text{Eu}(\text{dpa})_3^{3-}$ complexes used in this study have well-characterized spectroscopic and chiroptical properties that have been exploited in a number of CPL studies of chiral discrimination.^{31,32,34–36} In the absence of a chiral perturbation, excitation of the $\text{Eu}(\text{dpa})_3^{3-}$ complexes with unpolarized light produces a racemic excited state population. This in turn leads to equal intensities of left- vs right-circularly polarized light with $\Delta I(\lambda)$ and $g_{\text{em}}(\lambda) = 0$. When a chiral species is added that

disrupts the racemic equilibrium ($\Delta \leftrightarrow \Lambda$) of the $\text{Eu}(\text{dpa})_3^{3-}$ complexes, the CPL and g_{em} observed will be nonzero. Therefore, the sign and magnitude of g_{em} reflects the sense (i.e., handedness) and degree of chiral discrimination by the added chiral species, respectively. In the current study, the chiral perturbation arises from the interaction between the amino acid CIL solvent and the $\text{Eu}(\text{dpa})_3^{3-}$ complexes generating a nonracemic equilibrium. The CPL and g_{em} recorded in these studies are a direct measure of the chiral discrimination ability of the CILs. The temperature dependence of the dissymmetry factor, g_{em} , is measured in order to understand the thermodynamics of chiral discrimination by the CIL solvent. Results for these five amino acid CILs are compared and discussed in terms of the relationship between amino acid structures and their chiral discrimination ability.

■ EXPERIMENTAL SECTION

Preparation of Amino Acid CILs. All materials for preparation of the amino acid chiral ionic liquids, including lithium bis(trifluoromethanesulfonimide), amino acid methyl ester hydrogen chloride salts, L-alanine, and tetrabutylammonium hydroxide, were purchased from Sigma-Aldrich and used without further purification. The tetrabutylammonium L-alanate CIL was prepared according to literature procedures.¹³ The amino acid methyl ester CILs were prepared following a literature procedure,¹² where equimolar amounts of amino acid methyl ester-HCl and lithium bis(trifluoromethanesulfonimide) were dissolved in a minimal volume of water. The solution forms two layers, and the amino acid CIL layer is separated from the aqueous layer using a separatory funnel. The amino acid CIL layer is then heated (<60 °C) under vacuum until the water content measures <0.2% water by mass with a volumetric Karl Fischer titration (MetroOhm, Titrino Plus 870).

Sample Preparation. All of the starting materials for preparing the $\text{Eu}(\text{dpa})_3^{3-}$ samples, $\text{EuCl}_3 \cdot 6\text{H}_2\text{O}$, and 2,6-pyridinedicarboxylic acid were purchased from Sigma-Aldrich and used without further purification. The complexes were prepared by dissolving $\text{EuCl}_3 \cdot 6\text{H}_2\text{O}$ in water and adding 3 equiv of NaOH to precipitate $\text{Eu}(\text{OH})_3$, which was filtered and added to an aqueous solution containing 3 equiv of 2,6-pyridinedicarboxylic acid (dpaH_2). Three equivalents of tetrabutylammonium hydroxide (TBAOH) was added dropwise to this solution to precipitate $[\text{TBA}]_3\text{Eu}(\text{dpa})_3$. The water (solvent) was removed by heating under vacuum leaving an oily white solid. Samples were prepared by adding 0.5 mg of $[\text{TBA}]_3\text{Eu}(\text{dpa})_3$ to approximately 2.0 g of amino acid CILs and stirring under mild heat (<60 °C) for several hours until the complexes dissolve. At this sample concentration (0.18 mM), $\text{Eu}(\text{dpa})_3^{3-}$ dissolves easily in all of the amino acid CILs studied. Emission spectra of $\text{Eu}(\text{dpa})_3^{3-}$ complexes dissolved in CILs were recorded on a Perkin-Elmer LS-55 Luminescence spectrometer.

Measuring CPL. The CPL spectra are recorded on instrumentation assembled in our lab. A 450 W xenon arc lamp/0.10 m monochromator serves as the source of the excitation wavelength of 280 nm, which excites the dpa ligands to transfer energy to the Eu^{3+} (antenna effect).³⁷ The sample is held in a water-jacketed fluorescence cuvette controlled by a circulating water bath (Brinkmann rms Lauda) to maintain temperatures between 263 and 323 K. The circular polarization of the luminescence is selected using a photoelastic modulator (Hinds PEM-80) operating at 50 kHz in combination with a

Glan-Thomson linear polarizer. The emission wavelength is selected by a 0.32 m monochromator (Horiba Jobin Yvon iHR320) with a resolution of 0.06 nm and detected by a red-sensitive photomultiplier tube (Hamamatsu R928). The output from the PMT can be processed two different ways, including analogue capture and lock-in amplifier. Operating in analogue capture mode, the output from the PMT is sent to a digitizing oscilloscope to record the luminescence intensity, and the output of the PEM is also recorded to identify the polarization of the luminescence intensity. A computer program is used to average and store intensity and polarization information. In order to achieve good signal-to-noise ratios, spectra are typically signal averaged over several hours. Using the lock-in amplifier requires two measurements for each sample, one to measure the CPL using PEM output as the lock-in reference signal and a second measurement of the total luminescence using a mechanical chopper to pulse the excitation from the Xe lamp as the lock-in reference signal. The lock-in amplifier gives an improved signal-to-noise ratio over analogue capture, which means less signal averaging. Both analogue capture and lock-in amplifier methods give the same $g_{\text{em}}(\lambda)$ for $\text{Eu}(\text{facam})_3$ in DMSO (a CPL standard).³⁸

■ RESULTS AND DISCUSSION

In this study, chiral discrimination of the amino acid CILs is measured by their ability to perturb the equilibrium population of Λ - vs Δ - $\text{Eu}(\text{dpa})_3^{3-}$ from racemic to nonracemic. For $\text{Eu}(\text{dpa})_3^{3-}$ complexes, the emission spectrum of the 4f–4f transitions of Eu^{3+} can be used to ensure that the complexes are stable and inert to changes in the Eu^{3+} coordination environment when dissolved in the CILs. Figure 2 shows a comparison of the ${}^7\text{F}_{0-2} \leftarrow {}^5\text{D}_0$ region of the emission spectrum for $\text{Eu}(\text{dpa})_3^{3-}$ dissolved in $[\text{D-AlaC1}][\text{Tf}_2\text{N}]$ vs water. Figure 2 shows some clear differences in the spectra of

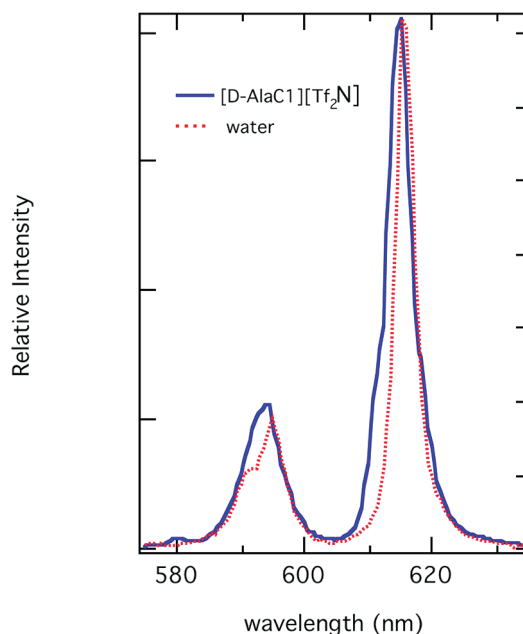


Figure 2. Emission spectra for the ${}^7\text{F}_{0-2} \leftarrow {}^5\text{D}_0$ region of $\text{Eu}(\text{dpa})_3^{3-}$ dissolved in water and $[\text{D-AlaC1}][\text{Tf}_2\text{N}]$. The emission spectra for $\text{Eu}(\text{dpa})_3^{3-}$ dissolved in the other amino acid CILs are not included because they are similar in shape and relative intensity to the spectra in $[\text{D-AlaC1}][\text{Tf}_2\text{N}]$.

$\text{Eu}(\text{dpa})_3^{3-}$ in $[\text{D-AlaC1}][\text{Tf}_2\text{N}]$ vs water. For example, the ${}^7\text{F}_0 \leftarrow {}^5\text{D}_0$ transition (~ 580 nm), forbidden in D_3 symmetry, is extremely weak but present in the $[\text{D-AlaC1}][\text{Tf}_2\text{N}]$. In the ${}^7\text{F}_1 \leftarrow {}^5\text{D}_0$ transition (~ 594 nm), there are two peaks in water, which appear as one broad peak and a small shoulder in the CILs. Overall, the peaks shown in Figure 2 seem to be broader in the CILs than in water. This may be a reflection of the strong Coulombic interaction between the cationic amino acid methyl ester(s) in the CIL solvent and the $\text{Eu}(\text{dpa})_3^{3-}$ complex. The observed energy level splittings and locations for the ${}^5\text{D}_0 \rightarrow {}^7\text{F}_{0,1,2}$ spectral regions shown in Figure 2 are similar for water vs CILs. This similarity along with the fact that it is unlikely that Tf_2N^- anions of the CILs would replace the dpa^{2-} ligands indicates that there is not a change in the coordination environment around the Eu^{3+} . Additionally, the luminescence lifetimes of the ${}^5\text{D}_0$ state of the $\text{Eu}(\text{dpa})_3^{3-}$ in the CILs show monoexponential decay with lifetimes between 1.71 and 2.03 ms that are constant over the 283–323 K temperature range of this study. These lifetimes are longer than those observed in aqueous solution³⁴ and demonstrate that water and the CILs are not significantly quenching the luminescence of $\text{Eu}(\text{dpa})_3^{3-}$ in the CILs. The combination of the luminescence spectra and lifetime data suggest that the coordination environment of $\text{Eu}(\text{dpa})_3^{3-}$ is stable, and there is an outer-sphere interaction between the $\text{Eu}(\text{dpa})_3^{3-}$ complexes and the CIL solvent.

CPL Spectra. Figures 3 and 4 show the CPL ($I_L - I_R$) and total luminescence ($I_L + I_R$) spectra for the ${}^5\text{D}_0 \rightarrow {}^7\text{F}_1$ spectrum

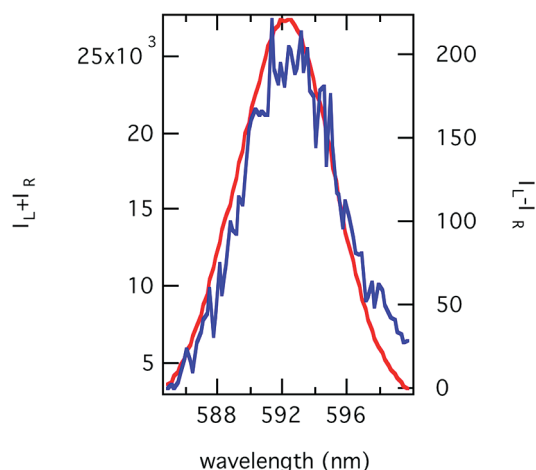


Figure 3. CPL and total luminescence spectrum of the ${}^5\text{D}_0 \rightarrow {}^7\text{F}_1$ region of $\text{Eu}(\text{dpa})_3^{3-}$ in $[\text{L-AlaC1}][\text{Tf}_2\text{N}]$ at 293 K.

of $\text{Eu}(\text{dpa})_3^{3-}$ dissolved in $[\text{L-AlaC1}][\text{Tf}_2\text{N}]$ and $[\text{D-AlaC1}][\text{Tf}_2\text{N}]$, respectively. The CPL spectra in Figures 3 and 4 show one broad peak centered at 593 nm with $g_{\text{em}}(593) = +0.013$ in $[\text{L-AlaC1}][\text{Tf}_2\text{N}]$ and $g_{\text{em}}(593) = -0.013$ in $[\text{D-AlaC1}][\text{Tf}_2\text{N}]$. Typically, the CPL spectrum of $\text{Eu}(\text{dpa})_3^{3-}$ in this region shows two peaks, located at 588 and 594 nm.³⁴ The fact that the 588 and 594 nm peaks are not fully resolved in the CPL spectra in Figures 3 and 4 (not shown, but it is also true for $[\text{L-LeuC1}][\text{Tf}_2\text{N}]$) which is another indication, along with Figure 2, of the strong solvation interaction between the $\text{Eu}(\text{dpa})_3^{3-}$ complexes and the CIL solvent. It is also significant that the g_{em} values have opposite signs for $[\text{L- vs D-AlaC1}][\text{Tf}_2\text{N}]$, which show that the preference (Λ vs Δ) of the discrimination is dictated by the stereochemistry of the alanine methyl ester cation.

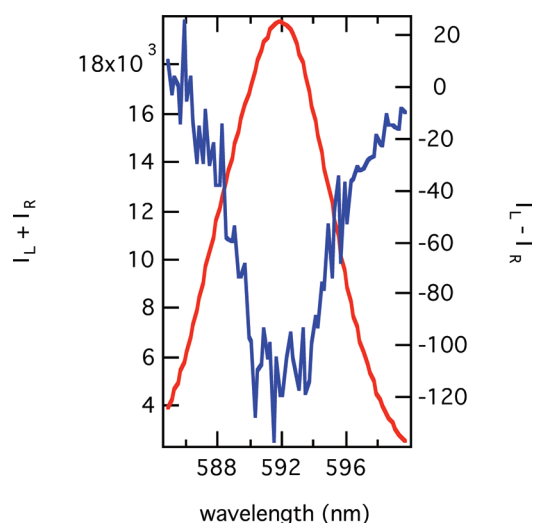


Figure 4. CPL and total luminescence spectrum of the ${}^5\text{D}_0 \rightarrow {}^7\text{F}_1$ region of $\text{Eu}(\text{dpa})_3^{3-}$ in $[\text{D-AlaC1}][\text{Tf}_2\text{N}]$ at 293 K.

Figures 5 and 6 show the CPL and total luminescence spectra for the ${}^5\text{D}_0 \rightarrow {}^7\text{F}_1$ and ${}^7\text{F}_2$ regions of $\text{Eu}(\text{dpa})_3^{3-}$

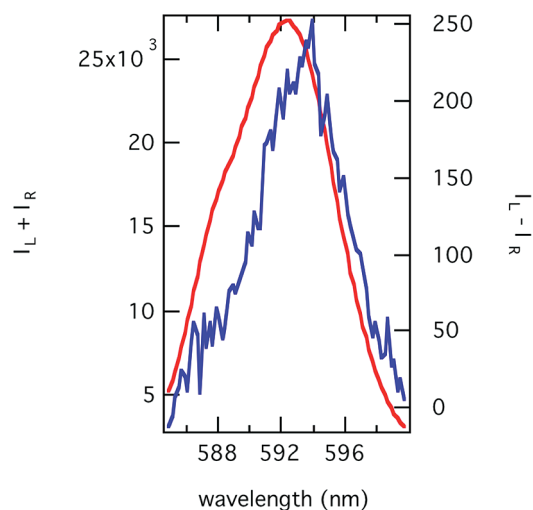


Figure 5. CPL and total luminescence spectrum of the ${}^5\text{D}_0 \rightarrow {}^7\text{F}_1$ region of $\text{Eu}(\text{dpa})_3^{3-}$ in $[\text{L-ProC1}][\text{Tf}_2\text{N}]$ at 293 K.

dissolved in $[\text{L-ProC1}][\text{Tf}_2\text{N}]$. In Figure 5, the CPL spectrum shows two positive peaks with $g_{\text{em}}(588) = +0.007$ and $g_{\text{em}}(594) = +0.012$, which is more typical for $\text{Eu}(\text{dpa})_3^{3-}$ than in the other amino acid CILs. Figure 6 shows one negative CPL peak with $g_{\text{em}}(614) = -0.006$. The relative magnitude and sign of the ${}^5\text{D}_0 \rightarrow {}^7\text{F}_1$ vs ${}^7\text{F}_2$ dissymmetry values are consistent with a nonracemic population of $\Lambda\text{-Eu}(\text{dpa})_3^{3-}$ vs $\Delta\text{-Eu}(\text{dpa})_3^{3-}$ observed in aqueous solutions.^{33,39} The magnitudes of these g_{em} values ($\sim 10^{-2}$) are relatively large for Λ - vs $\Delta\text{-Eu}(\text{dpa})_3^{3-}$ studies and are comparable to values from enantioselective quenching measurements³³ and Pfeiffer effect studies by adding chiral species to perturb the racemization equilibrium.³⁹ The CPL and emission spectra shown in Figures 2–6 and the monoexponential luminescence decays indicate that the g_{em} values observed are not the result of enantioselective quenching or changes in the rotatory strength of $\Lambda\text{-Eu}(\text{dpa})_3^{3-}$ vs $\Delta\text{-Eu}(\text{dpa})_3^{3-}$ but are due to the formation of a nonracemic (i.e., enantioenriched) population from differential diastereomeric

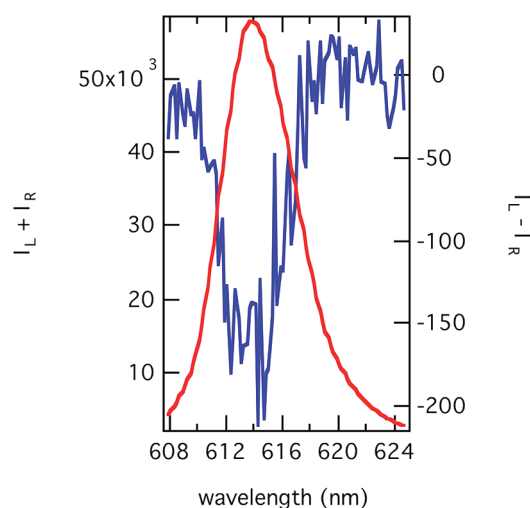


Figure 6. CPL and total luminescence spectrum of the $^5D_0 \rightarrow ^7F_2$ region of $\text{Eu}(\text{dpa})_3^{3-}$ in $[\text{L-ProC1}][\text{Tf}_2\text{N}]$ at 293 K.

interactions between the enantiomers of the chiral complex and the amino acid CIL solvents.

Temperature Dependent Chiral Discrimination. One of the main reasons to study chiral ionic liquids in chiral discrimination processes is that they offer the structural flexibility of the components of the ionic liquid to tailor their chiral discrimination properties. In an effort to investigate the impact of structure, this study examined the chiral discrimination by five amino acid based CILs (shown in Table 1). Four of the CILs differ only by the choice of amino acid methyl ester cation: L-leucine methyl ester, L-proline methyl ester, and L- and D-alanine methyl ester. Table 2 shows the dissymmetry values

Table 2. Temperature Dependent g_{em} Values for $\text{Eu}(\text{dpa})_3^{3-}$ Dissolved in Amino Acid CILs over the 283–323 K Range

T (K)	$g_{\text{em}}(\lambda)^a$ [L-AlaC1] [Tf ₂ N]	$g_{\text{em}}(\lambda)^a$ [D-AlaC1] [Tf ₂ N]	$g_{\text{em}}(\lambda)^a$ [L-LeuC1] [Tf ₂ N]	$g_{\text{em}}(\lambda)^a$ [L-ProC1] [Tf ₂ N]	$g_{\text{em}}(\lambda)^a$ [L-TBA] [Ala]
283	+0.018	−0.015	+0.011	+0.016	n.d. ^b
293	+0.013	−0.013	+0.011	+0.012	0
298	+0.012	−0.008	+0.010	+0.011	n.d. ^b
303	+0.011	−0.006	+0.009	+0.011	
308	+0.011	−0.006	+0.010	+0.011	
313	+0.009	−0.005	+0.010	+0.010	
318	+0.009	−0.004	+0.011	+0.010	
323	+0.009	−0.005	+0.010	+0.007	

^a g_{em} reported at maximum of $^5D_0 \rightarrow ^7F_1$ transition ($\lambda = 594$ or 593 nm). ^bn.d. = not determined.

measured in all five CILs over 283–323 K temperature range. The g_{em} value measured for TBA/L-Ala is near zero because the europium complexes are anions and will more closely interact with TBA^+ and not the chiral amino acid anion. The data in Table 2 show that the sign of the g_{em} corresponds to the stereochemistry of the amino acid methyl ester, where L-enantiomers give positive g_{em} and D-enantiomers give negative g_{em} values. A previous study by Coruh et al., based on comparisons with resolved $\text{Eu}(\text{oda})_3^{3-}$ (where oda = oxidiacetate dianion), have assigned $g_{\text{em}}(594) > 0$ to an excess of Λ and $g_{\text{em}}(594) < 0$ to an excess of the Δ - $\text{Eu}(\text{dpa})_3^{3-}$ enantiomer.⁴⁰ Assuming these enantiomeric assignments, the data in Table 2 shows that the L-amino acid methyl ester CILs

shifts the equilibrium toward the Λ enantiomer, while D-alanine methyl ester CIL shifts the equilibrium toward the Δ enantiomer.

The magnitudes of g_{em} in Table 2 and the degree of chiral discrimination by the CILs show variability based on temperature and identity of the CIL. The chiral discrimination observed in these measurements is the result of a shift in the racemization equilibrium of the $\text{Eu}(\text{dpa})_3^{3-}$ complexes by the CILs. The measured dissymmetry factors shown in Table 2 are expressed in terms of the excited state enantiomeric excess (η^*) by the following equation

$$g_{\text{em}}(\lambda) = \eta^* g_{\text{em}}^{\Lambda}(\lambda) \quad (2)$$

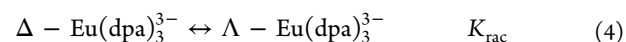
where $g_{\text{em}}^{\Lambda}(\lambda)$ is the dissymmetry factor of an enantiomerically resolved Λ - $\text{Eu}(\text{dpa})_3^{3-}$ excited state population, and the enantiomeric excess is expressed as

$$\eta^* = \frac{[\Lambda]^* - [\Delta]^*}{[\Lambda]^* + [\Delta]^*} = \frac{g_{\text{em}}(\lambda)}{g_{\text{em}}^{\Lambda}(\lambda)} \quad (3)$$

where $[\Lambda]^*$ and $[\Delta]^*$ are the concentrations of each of the $\text{Eu}(\text{dpa})_3^{3-}$ enantiomers, respectively. Assuming that there is no enantioselective quenching of the excited state europium complexes in the amino acid CILs, the ground and excited state enantiomeric excess values are identical (i.e., $\eta = \eta^*$). Therefore, results from these emission measurements are directly related to the chiral discrimination by the CILs to the ground state population of $\text{Eu}(\text{dpa})_3^{3-}$.

In order to find the enantiomeric excess using eq 3, a value for $g_{\text{em}}^{\Lambda}(\lambda)$ is necessary, but it is impossible to directly measure the value due to the racemization that occurs.³⁰ However, enantioselective quenching measurements with resolved cobalt diaminocyclohexane complexes make it possible to determine a value of $g_{\text{em}}^{\Lambda}(\lambda) = 0.29$ for $\text{Eu}(\text{dpa})_3^{3-}$.⁴¹ Assuming that the rotatory strengths of the transitions in $\text{Eu}(\text{dpa})_3^{3-}$ are unaffected by the solvent (water vs CIL), this $g_{\text{em}}^{\Lambda}(\lambda)$ value can be substituted into eq 3 to determine an enantiomeric excess, η , in the amino acid CILs. The temperature dependent enantiomeric excess (η) ratios for $\text{Eu}(\text{dpa})_3^{3-}$ dissolved in the amino acid methyl ester CILs are shown in Figure 7. For [L-AlaC1][Tf₂N] vs [D-AlaC1][Tf₂N], η has the opposite sign, and the magnitude of η is larger for [L-AlaC1][Tf₂N] at every temperature. The enantiomeric excesses in [L-ProC1][Tf₂N], [L-AlaC1][Tf₂N], and [D-AlaC1][Tf₂N] all decrease with increasing temperature. The data show a 6% enantiomeric excess of Λ - $\text{Eu}(\text{dpa})_3^{3-}$ at 283 K for both [L-ProC1][Tf₂N] and [L-AlaC1][Tf₂N] that decreases down to less than 4% at 323 K. In contrast, the enantiomeric excess, η , is constant (within experimental uncertainty) over the entire temperature range for the [L-LeuC1][Tf₂N] ionic liquid.

Thermodynamic Analysis of Chiral Discrimination. The chiral discrimination by the CILs can also be expressed as a racemization equilibrium:



Rearranging and substituting eqs 2 and 3 into the equilibrium expression gives an equilibrium constant that can be written as

$$K_{\text{rac}} = \frac{1 + \eta}{1 - \eta} \quad (5)$$

Substituting the temperature dependent enantiomeric excesses, η , from Figure 7 into eq 5 gives the racemization

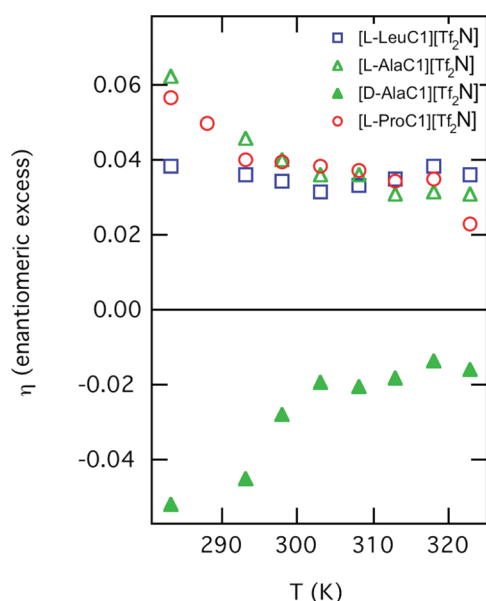


Figure 7. Enantiomeric excess (η) vs temperature for $\text{Eu}(\text{dpa})_3^{3-}$ dissolved in $[\text{L-ProC1}][\text{Tf}_2\text{N}]$, $[\text{L-AlaC1}][\text{Tf}_2\text{N}]$, $[\text{L-LeuC1}][\text{Tf}_2\text{N}]$, and $[\text{D-AlaC1}][\text{Tf}_2\text{N}]$ over the 283–323 K range.

equilibrium constants, K_{rac} , with a temperature dependence that can be expressed in the van't Hoff equation

$$\ln K_{\text{rac}} = -\frac{\Delta H_{\text{rac}}}{RT} + \frac{\Delta S_{\text{rac}}}{T} \quad (6)$$

where R is the gas constant and ΔH_{rac} and ΔS_{rac} are the enthalpy and entropy of racemization. In these studies the enthalpy of racemization in eq 6 represents the strength of the chiral discriminatory interactions (e.g., Coulombic, H-bonding) between the CILs and the $\text{Eu}(\text{dpa})_3^{3-}$ complexes.

Figure 8 shows a van't Hoff plot ($\ln K_{\text{rac}}$ vs $1/T$) of the racemization equilibrium constants for $\text{Eu}(\text{dpa})_3^{3-}$ in $[\text{L-AlaC1}][\text{Tf}_2\text{N}]$, $[\text{D-AlaC1}][\text{Tf}_2\text{N}]$, $[\text{L-LeuC1}][\text{Tf}_2\text{N}]$, and $[\text{L-ProC1}][\text{Tf}_2\text{N}]$ CILs. For the $[\text{L-AlaC1}][\text{Tf}_2\text{N}]$, $[\text{D-AlaC1}][\text{Tf}_2\text{N}]$, and $[\text{L-ProC1}][\text{Tf}_2\text{N}]$ data, the plots are clearly not linear over the entire temperature range, indicating that the enthalpy of racemization (ΔH_{rac}) is not constant over this temperature range. However, these three CILs do show linearity above 293–298 K, and lines representing fits to eq 6 of the high temperature region (298–323 K) are shown in Figure 8. Fits of the data to eq 6 give $\Delta H_{\text{rac}} = -0.7 \pm 0.2$ kJ/mol for $[\text{L-AlaC1}][\text{Tf}_2\text{N}]$ and $[\text{L-ProC1}][\text{Tf}_2\text{N}]$ and $\Delta H_{\text{rac}} = +0.7 \pm 0.2$ kJ/mol for $[\text{D-AlaC1}][\text{Tf}_2\text{N}]$. Considering that the sign of ΔH_{rac} is simply an indicator of which enantiomer ($\Lambda\text{-Eu}(\text{dpa})_3^{3-}$ or $\Delta\text{-Eu}(\text{dpa})_3^{3-}$) is favored, $[\text{L-AlaC1}][\text{Tf}_2\text{N}]$, $[\text{D-AlaC1}][\text{Tf}_2\text{N}]$, and $[\text{L-ProC1}][\text{Tf}_2\text{N}]$ CILs show identical chiral discriminatory interaction strengths, $|\Delta H_{\text{rac}}|$ over this temperature range. These results suggest that structural differences between $[\text{AlaC1}^+]$ and $[\text{ProC1}^+]$ do not play a critical role in the chiral discrimination. Below 298 K there is not enough data to quantitatively determine the low temperature ΔH_{rac} but it is clear from Figure 8 that the enthalpy is larger at the low temperatures than it is at higher temperatures. All of this data is consistent with chiral discrimination that derives from intermolecular interactions (e.g., Coulombic and/or hydrogen bonding) between amino acid methyl ester cations in the CIL and the $\text{Eu}(\text{dpa})_3^{3-}$ enantiomers.

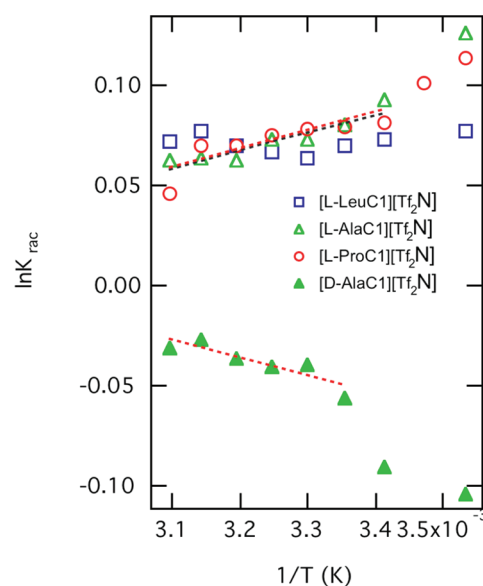


Figure 8. Plot of $\ln K_{\text{rac}}$ vs $1/T$ for $\text{Eu}(\text{dpa})_3^{3-}$ dissolved in $[\text{L-ProC1}][\text{Tf}_2\text{N}]$, $[\text{L-AlaC1}][\text{Tf}_2\text{N}]$, $[\text{L-LeuC1}][\text{Tf}_2\text{N}]$, and $[\text{D-AlaC1}][\text{Tf}_2\text{N}]$ over the 283–323 K range. Dotted lines show fits to the van't Hoff equation over a portion of the data for $[\text{L-ProC1}][\text{Tf}_2\text{N}]$, $[\text{L-AlaC1}][\text{Tf}_2\text{N}]$, and $[\text{D-AlaC1}][\text{Tf}_2\text{N}]$.

Among the four amino acid methyl ester CILs studied, the $[\text{L-LeuC1}][\text{Tf}_2\text{N}]$ data are unique. Fits of the data to eq 6 in Figure 8 for $[\text{L-LeuC1}][\text{Tf}_2\text{N}]$ over the entire temperature range give an enthalpy of racemization, ΔH_{rac} , equal to zero. It is important to note that this does not imply that there are no enthalpic interactions (i.e., Coulombic, etc.) between $[\text{L-LeuC1}^+]$ and $\text{Eu}(\text{dpa})_3^{3-}$, but that the interactions are not enantioselective. However, an enantiomeric excess of 4% (Figure 7) $\Lambda\text{-Eu}(\text{dpa})_3^{3-}$ is observed in $[\text{L-LeuC1}][\text{Tf}_2\text{N}]$, which is due entirely to entropic chiral discrimination effects. At higher temperatures, this entropic chiral discrimination is larger than the enthalpic chiral discrimination observed in the other amino acid CIL solvents.

This result implies that a degree of chiral ordering is imposed by the $[\text{L-LeuC1}][\text{Tf}_2\text{N}]$ on the solvated $\text{Eu}(\text{dpa})_3^{3-}$ complexes independent of direct ion–ion interactions. A study by Seddon et al. showed that the mixing behavior of ionic liquids with ionic liquids is entropically driven based on matching ionic sizes rather than enthalpic ion–ion interactions.⁴² Welton et al. also observed ideal mixing behavior (entropically dominated) when Kosower's salt was dissolved in imidazolium-based ionic liquids.⁴³ The data in this study do not clearly indicate why $[\text{L-LeuC1}][\text{Tf}_2\text{N}]$ is the only amino acid CIL that demonstrates entropically dominated chiral discrimination, but the size of $[\text{L-LeuC1}^+]$ may be playing an important role. Of the amino acid methyl ester cations used in this study, $[\text{L-LeuC1}^+]$ is largest and closest to the size of tetrabutylammonium ions, $[\text{TBA}^+]$, from the $[\text{TBA}]_3\text{Eu}(\text{dpa})_3$ salt. The ionic size matching and the lack of enthalpic chiral discrimination interactions could be the source of the chiral ordering provided by the $[\text{L-LeuC1}][\text{Tf}_2\text{N}]$ solvent.

CONCLUSION

Chiral discrimination is observed in four of the amino acid based CILs in this study. These four CILs represent two enantiomers (L vs D) and three nonpolar amino acid methyl ester structures. The chiroptical results show that the

preference of the chiral discrimination is directly related to the handedness of the amino acid methyl ester cation, but the magnitude of discrimination defies simple description. As expected, the chiral discrimination is due to enthalpic interactions between the cation in the CIL and the europium anionic complexes in $[L\text{-AlaCl}^+]$, $[D\text{-AlaCl}^+]$, and $[L\text{-ProCl}^+]$, but the results also indicate an indifference to the structural variation of these ions (i.e., methyl $-R$ group vs rigid cyclic). The results for $[L\text{-LeuCl}^+]$ differ significantly from the other CILs. The leucine methyl ester has the largest side chain (isobutyl $-R$ group), which seems to eliminate any enthalpic chiral discriminatory interactions. In the absence of these enthalpic interactions, $[L\text{-LeuCl}][\text{Tf}_2\text{N}]$ demonstrates an entirely entropic chiral discrimination.

The potential benefit of chiral ionic liquids is the ability to synthetically control the chiral discrimination properties by choice of cations and anions. The results from this study present a mixed message about the ability to control chiral discrimination by amino acid methyl ester based CILs. The amino acid CILs do provide control over the preference of the chiral discrimination and demonstrate enantiomeric excesses in the europium complexes that are comparable to those achieved through the addition of chiral resolving agents.³⁹ However, these results suggest (at least for these dissymmetric europium complexes) that it is difficult to establish a simple relationship between the magnitude of chiral discrimination and the amino acid structure.

AUTHOR INFORMATION

Corresponding Author

*E-mail: tahopkin@butler.edu.

Notes

The authors declare no competing financial interest.

ACKNOWLEDGMENTS

We thank Matt Goldey for writing the instrument software and Eric Shoemaker for preliminary measurements. We also thank the Butler Summer Institute and the Butler Institute for Research and Scholarship for financial support.

REFERENCES

- Baudequin, C.; Bregeon, D.; Levillain, J.; Guillen, F.; Plaquevent, J. C.; Gaumont, A. C. *Tetrahedron: Asymmetry* **2005**, *16*, 3921.
- Bica, K.; Gaertner, P. *Eur. J. Org. Chem.* **2008**, 3235.
- Gaumont, A. C.; Genisson, Y.; Guillen, F.; Plaquevent, J. C. *Actual Chim.* **2011**, 84.
- Ding, J.; Armstrong, D. W. *Chirality* **2005**, *17*, 281.
- Kagimoto, J.; Fukumoto, K.; Ohno, H. *Chem. Commun.* **2006**, 2254.
- Weingartner, H. *Angew. Chem., Int. Ed.* **2008**, *47*, 654.
- Bonanni, M.; Soldaini, G.; Faggi, C.; Goti, A.; Cardona, F. *Synlett* **2009**, 747.
- Bregeon, D.; Levillain, J.; Guillen, F.; Plaquevent, J. C.; Gaumont, A. C. *Amino Acids* **2008**, *35*, 175.
- Malhotra, S. V.; Wang, Y.; Kumar, V. *Lett. Org. Chem.* **2009**, *6*, 264.
- Nageshwar, D.; Rao, D. M.; Acharyulu, P. V. R. *Synth. Commun.* **2009**, *39*, 3357.
- de Rooy, S. L.; Li, M.; Bwambok, D. K.; El-Zahab, B.; Challa, S.; Warner, I. M. *Chirality* **2011**, *23*, 54.
- Tao, G. H.; He, L.; Sun, N.; Kou, Y. *Chem. Commun.* **2005**, 3562.
- Jiang, Y. Y.; Wang, G. N.; Zhou, Z.; Wu, Y. T.; Geng, J.; Zhang, Z. B. *Chem. Commun.* **2008**, 505.
- Ohno, H.; Fukumoto, K. *Acc. Chem. Res.* **2007**, *40*, 1122.
- Berthod, A.; He, L.; Armstrong, D. W. *Chromatographia* **2001**, *53*, 63.
- Ding, J.; Welton, T.; Armstrong, D. W. *Anal. Chem.* **2004**, *76*, 6819.
- Shamsi, S. A.; Danielson, N. D. *J. Sep. Sci.* **2007**, *30*, 1729.
- Tang, F.; Zhang, Q. L.; Ren, D. D.; Nie, Z.; Liu, Q. A.; Yao, S. Z. *J. Chromatogr., A* **2010**, *1217*, 4669.
- Chen, D. J.; Schmitkamp, M.; Francio, G.; Klankermayer, J.; Leitner, W. *Angew. Chem., Int. Ed.* **2008**, *47*, 7339.
- Gadenne, B.; Hesemann, P.; Moreau, J. J. E. *Tetrahedron Lett.* **2004**, *45*, 8157.
- Malhotra, S. V.; Kumar, V.; Parmar, V. S. *Curr. Org. Synth.* **2007**, *4*, 370.
- Qian, Y. B.; Zheng, X.; Wang, Y. M. *Eur. J. Org. Chem.* **2010**, 3672.
- Warner, I. M.; Bwambok, D. K.; Marwani, H. M.; Fernand, V. E.; Fakayode, S. O.; Lowry, M.; Negulescu, I.; Strongin, R. M. *Chirality* **2008**, *20*, 151.
- Liu, Q.; Wu, K. K.; Tang, F.; Yao, L. H.; Yang, F.; Nie, Z.; Yao, S. Z. *Chem.—Eur. J.* **2009**, *15*, 9889.
- Zhao, H.; Jackson, L.; Song, Z. Y.; Olubajo, O. *Tetrahedron: Asymmetry* **2006**, *17*, 1549.
- Chen, X. W.; Li, X. H.; Hu, A. X.; Wang, F. R. *Tetrahedron: Asymmetry* **2008**, *19*, 1.
- Xu, D. Z.; Liu, Y. J.; Shi, S.; Wang, Y. M. *Tetrahedron: Asymmetry* **2010**, *21*, 2530.
- Wasserscheid, P.; Bosmann, A.; Bolm, C. *Chem. Commun.* **2002**, 200.
- Warner, I. M.; de Rooy, S. L.; Li, M.; Bwambok, D. K.; El-Zahab, B.; Challa, S. *Chirality* **2011**, *23*, 54.
- Glover-Fischer, D. P.; Metcalf, D. H.; Hopkins, T. A.; Pugh, V. J.; Chisdes, S. J.; Richardson, F. S. *Inorg. Chem.* **1998**, *37*, 3026.
- Muller, G.; Riehl, J. P. *J. Fluoresc.* **2005**, *15*, 553.
- Moussa, A.; Pham, C.; Bommireddy, S.; Muller, G. *Chirality* **2009**, *21*, 497.
- Metcalf, D. H.; Snyder, S. W.; Demas, J. N.; Richardson, F. S. *J. Am. Chem. Soc.* **1990**, *112*, 5681.
- Hopkins, T. A.; Metcalf, D. H.; Richardson, F. S. *Chirality* **2008**, *20*, 511.
- Meskers, S. C. J.; Dekkers, H. P. J. M. *J. Phys. Chem. A* **2001**, *105*, 4589.
- Huskowska, E.; Gawryszewska, P.; Legendziewicz, J.; Maupin, C. L.; Riehl, J. P. *J. Alloys Compd.* **2000**, *303*, 325.
- Bunzli, J. C. G.; Piguet, C. *Chem. Soc. Rev.* **2005**, *34*, 1048.
- Castiglioni, E.; Abbate, S.; Longhi, G. *Appl. Spectrosc.* **2010**, *64*, 1416.
- Huskowska, E.; Riehl, J. P. *Inorg. Chem.* **1995**, *34*, 5615.
- Coruh, N.; Hilmes, G. L.; Riehl, J. P. *Inorg. Chem.* **1988**, *27*, 3647.
- Bolender, J. P.; Richardson, F. S. *Biophys. Chem.* **2003**, *105*, 293.
- Arce, A.; Earle, M. J.; Katdare, S. P.; Rodriguez, H.; Seddon, K. R. *Chem. Commun.* **2006**, 2548.
- Hallett, J. P.; Lui, M. Y.; Crowhurst, L.; Hunt, P. A.; Niedermeyer, H.; Welton, T. *Chem. Sci.* **2011**, *2*, 1491.